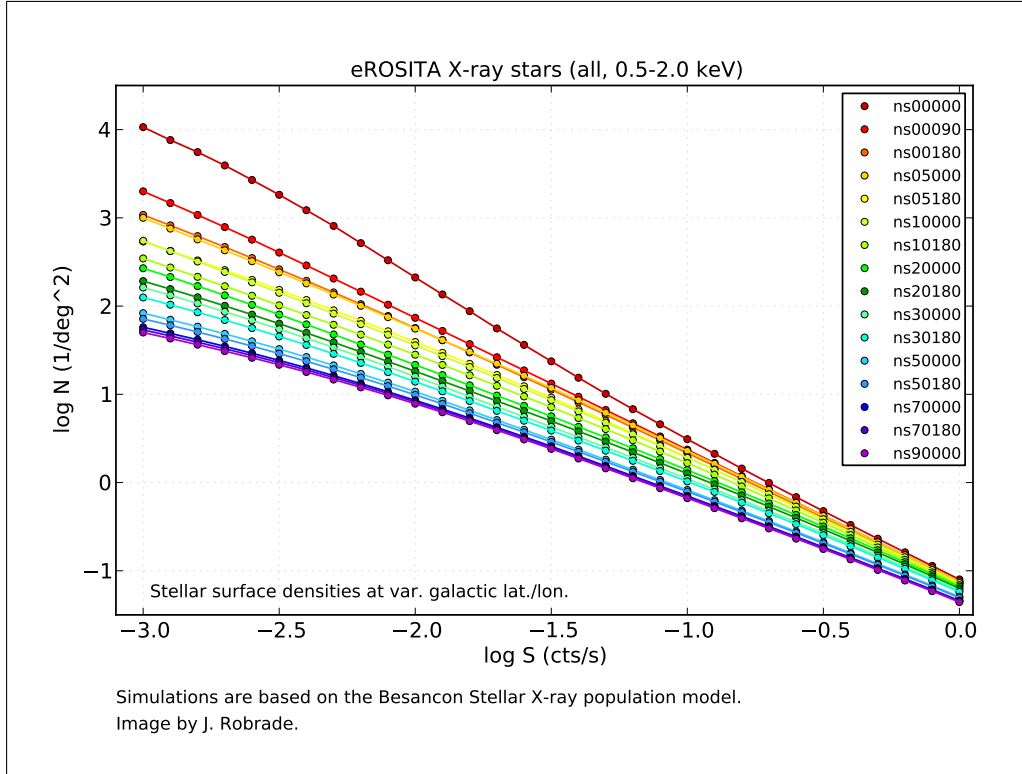


Stars in the eROSITA all-sky survey:

Results from the Besancon Stellar X-ray population model

One of the basic questions regarding stellar science is: How many stars will eROSITA detect?



In this study we use the 'Besancon Stellar X-ray population model' (Guilout et al., 1996) to estimate the stellar surface densities for the eROSITA all-sky survey. The above figure summarizes the main outcome of this simulation and shows the cumulative distributions of magnetically active stars at various galactic directions; plotted are the mean surface densities vs. the flux sensitivity of eROSITA observations at various galactic directions. Summing up, we expect roughly 0.7×10^6 stellar sources in the final eRASS catalog.

The Besancon model subdivides the stellar population into three age bins, namely 'Pleiades': 0–150 Myr, 'Hyades': 150 Myr–1 Gyr and 'Old Disk': 1–10 Gyr. Stars are further subdivided into six spectral type (mass) bins denoted as A, F, G, K, M, R (M5–M9). Surface densities were calculated for 16 galactic directions and a grid of sensitivity limits in $\log N/\log S$ space. The respective directions are given in the 'ns code', here the first two digits denote galactic latitude, the other three galactic longitude. All results refer to the full 4 yr eROSITA all-sky survey (eRASS8) if not specified otherwise.

Stellar X-ray luminosity functions are converted to count rates by using eROSITA ECFs derived from spectral modelling of single and multiple-temperature thermal plasma models using a FOV averaged response function. Stellar surface densities are given in $\log N$ [$1/\text{deg}^2$], fluxes are in $\log S$ [ctss^{-1}]. The spatial distributions are calculated for the 0.5–2.0 keV band, where most of the stellar X-ray emission is detected by eROSITA.

In the following we adopt for simplicity a homogeneous all-sky survey sensitivity of $\log S = -1.9$ [ctss^{-1}], corresponding to a detection limit of about 20 counts in 1600 s effective exposure time (The true detection limit is with 13–15 cts lower, however the true effective area at

energies below 1.0 keV is also about 25 % lower compared to the older ARF-files used in the simulation. Overall these effects roughly compensate.). The detection limit translates into an energy flux sensitivity of about 1×10^{-14} erg cm $^{-2}$ s $^{-1}$ at 0.3–5.0 keV energies. This is valid for coronal temperatures in the 2–10 MK range, i.e. thermal plasma models with 0.2–1.0 keV and current RMFs with FOV averaged ARFs. Tabulated stellar surface densities and star counts for different flux sensitivities are given in the appendix.

Notes on X-ray stars:

The predicted total number of stars is about 0.7 million, but it is important to mention that changes in survey efficiency e.g. due to source detection algorithms, background or in-orbit performance will have strong effects on the total number of detected stars and shifts by 30 % in either direction are easily possible. In addition, limitations in the stellar population models add to the overall uncertainty .

The stellar surface density increases from about 6 stars/deg 2 in polar regions, over 10 stars/deg 2 at intermediate latitudes (30° – 50°), up to 70 stars/deg 2 in the galactic disk. The stellar log N distributions have only a marginal dependence in longitudinal direction outside the galactic disk-region, roughly 10 % at 30° – 50° latitude and decreasing towards the poles. The situation differs in the disk, where the simulation predict values between 30 and 40 stars/deg 2 at 5° latitude, while at 0° latitude the surface density increases from 40 stars/deg 2 (gal. lon. = 180°) over 50 stars/deg 2 (gal. lon. = 90°/270°) up to 135 stars/deg 2 towards the direction of the galactic center.

The contributions from stars in the three age bins are similar, when taking the all-sky average (37 %, 38 %, 25 % are in the age-groups 1-3), but a strong latitudinal dependence of the age distribution is present. Within the disk-region (0° – 5° bins) young stars dominate strongly (68 %, 21 %, 11 % are in the age-groups 1-3), while at intermediate latitudes (10° – 50° bins: 24 %, 45 %, 31 %) and especially at higher latitudes a larger fraction of older stars is present (70° – 90° bins: 4 %, 49 %, 47 %). However, the covered period of the age bins in absolute time significantly differs (1:6:60) and one has to put these numbers into perspective.

Concerning the all-sky average of contributions from different stellar spectral types the simulations predicts for A, F, G, K, M, R (M5-M9) fractions of 0.014, 0.114, 0.203, 0.212, 0.451 and 0.007 respectively. Thus about 45 % of the X-ray detected stars are expected to be low mass stars of spectral type M, about 20 % each are G and K stars and about 10 % are F stars. In contrast to the age, the latitudinal dependence for the spectral type distribution is quite weak. Since the X-ray telescopes do not resolve multiple systems in many cases, stellar binarity is included in the XLF distributions. The population model does not include evolved active binaries like RSCVn systems, which need to be added. They will shift the distribution towards G and K type stars and might add in total 10–20 %, but their spatial distribution is not well known.

Notes on the stellar population model:

The simulation includes all 'normal' coronally active stars, i.e. the spectral types A–M, where X-ray emission is generated by magnetic activity. These stars will make up the bulk of X-ray stars in eROSITA data. However, many more exotic types of stellar sources are not included in the simulation. These are rare by number but often X-ray bright and include O and B stars as well as stellar systems involving a compact component like CVs, LMXB/HMXBs. Furthermore, the model does not account for local 'galactic inhomogeneities' like star formation regions etc.

Notes on the sky division:

The galactic disc at very low latitudes ($\lesssim 2$ deg) is divided into four longitudinal regions

(quarter-skies) with the $\log N$ -values at 90° and 270° being identical. At intermediate and higher latitudes the sky is divided into two latitudinal regions (half-skies) and one polar region is used. The latitudinal bins used are: $0^\circ - 2^\circ$ (ns=00), $2^\circ - 7^\circ$ (ns=05), $7^\circ - 15^\circ$ (ns=10), $15^\circ - 25^\circ$ (ns=20), $25^\circ - 40^\circ$ (ns=30), $40^\circ - 60^\circ$ (ns=50), $60^\circ - 80^\circ$ (ns=70), $80^\circ - 90^\circ$ (ns=90). In each case the value of the corresponding simulation is taken as the surface density of the respective sky-field.

Notes on the energy band:

Virtually all eROSITA stars will be detected in the 0.5–2.0 keV band. The number of stars that will be detected only in the soft (0.3–0.5 keV) or hard (2.0–5.0 keV) band is expected to be rather small; most of these sources will probably be either nearby weakly active stars (soft) or heavily absorbed sources in star-forming regions (hard). The fraction of photons from a typical star in the soft band is 10–25 %, those in the hard band is at maximum a few percent. Note that the final threshold and sensitivity at low energies is still uncertain. We adopt the simulated 0.5–2.0 keV band and treat it as the 'full' eROSITA band.

Notes on the stellar ECFs:

Stellar ECFs (ECF = flux / count rate) depend on the respective spectra and energy band. For a typical X-ray star they are about 1.3×10^{-12} erg cm⁻² s⁻¹ / cts s⁻¹ adopting the 0.3–5.0 keV band. The ECFs are with deviations of about ± 10 % quite stable in the 0.2–1.0 keV plasma temperature range, i.e. for most stellar spectra. Significant changes only occur for very soft ($kT \lesssim 0.1$ keV) and heavily absorbed ($\log N_{\text{H}} \gtrsim 22$ cm⁻²) sources.

Notes on the survey sensitivity:

The adopted exposure time of 1600 s is the approximate mean exposure time around the ecliptic equator. While this is the region with the lowest eRASS exposure, it assumes 100 % observing efficiency over four years of survey data taking and a 100 % detection efficiency for sources with $\gtrsim 20$ counts. The average exposure for the full sky is around 2.5 ks and 2 ks when ignoring the deeper exposed regions at the survey poles. However, the regions where stellar surface densities are high, specifically the galactic disk, have low to moderate exposure times in the eRASS. Using simulated exposure maps as sensitivity input induces shifts between spatial regions, but the total number of X-ray stars is approximately conserved.

Analysis, visualization and document by J. Robrade, simulations by P. Guillout with input from A. Schwobe and I. Traulsen. Electronically readable data is available on request.

Contact: jrobrade@hs.uni-hamburg.de

Appendix:

lim. Fx [erg cm ⁻² s ⁻¹]	5e-15	1e-14	5e-14	1e-13	5e-13
Sector /area [deg ²]	stars per deg ² / sector				
ns00000 / 359.93	516.7 / 185966.9	135.5 / 48766.7	6.79 / 2442.3	2.12 / 761.5	0.16 / 58.3
ns00090 / 719.86	145.7 / 104852.5	52.25 / 37610.8	4.70 / 3384.2	1.67 / 1203.1	0.15 / 108.0
ns00180 / 359.93	105.1 / 37821.7	41.06 / 14780.2	4.20 / 1511.0	1.54 / 554.8	0.14 / 52.0
ns05000 / 1793.89	100.8 / 180814.9	41.12 / 73760.7	4.45 / 7976.4	1.63 / 2925.0	0.15 / 268.8
ns05180 / 1793.89	68.2 / 122313.9	29.49 / 52906.7	3.64 / 6529.8	1.40 / 2516.2	0.14 / 250.3
ns10000 / 2824.80	62.4 / 176366.1	27.08 / 76504.1	3.52 / 9947.4	1.39 / 3939.9	0.14 / 401.7
ns10180 / 2824.80	47.5 / 134161.2	21.54 / 60832.1	3.01 / 8512.8	1.23 / 3469.7	0.13 / 375.6
ns20000 / 3378.62	36.7 / 123851.1	16.52 / 55828.9	2.45 / 8268.8	1.04 / 3511.0	0.13 / 423.1
ns20180 / 3378.62	30.2 / 102160.8	14.11 / 47665.3	2.20 / 7449.4	0.95 / 3212.9	0.12 / 399.9
ns30000 / 4541.34	26.5 / 120147.2	12.25 / 55621.7	1.91 / 8673.7	0.84 / 3800.2	0.11 / 500.5
ns30180 / 4541.34	22.7 / 103084.6	10.82 / 49141.7	1.76 / 8010.1	0.78 / 3554.5	0.11 / 478.4
ns50000 / 4604.66	17.0 / 78418.7	8.42 / 38770.2	1.39 / 6423.0	0.63 / 2903.4	0.09 / 416.6
ns50180 / 4604.66	15.5 / 71226.0	7.79 / 35860.9	1.33 / 6120.3	0.61 / 2789.0	0.09 / 405.5
ns70000 / 2450.02	13.2 / 32386.7	6.80 / 16657.1	1.19 / 2905.1	0.54 / 1326.2	0.08 / 197.9
ns70180 / 2450.02	12.6 / 30901.4	6.54 / 16030.5	1.16 / 2837.7	0.53 / 1300.7	0.08 / 195.3
ns90000 / 626.63	12.0 / 7515.5	6.26 / 3924.1	1.12 / 701.1	0.51 / 321.3	0.08 / 48.6
Total	1611989	684662	91693	38089	4581